



*Conference Proceedings of the 5th Asia Pacific Luminescence and Electron Spin Resonance Dating Conference
October 15th-17th, 2018, Beijing, China*

Guest Editor: Grzegorz Adamiec

THE BLEACHING OF DIFFERENT K-FELDSPAR pIRIR SIGNALS OF SOURCE MATERIALS OF LACUSTRINE SEDIMENT – A CASE STUDY FROM BOSTEN LAKE BASIN IN ARID CENTRAL ASIA

HE YANG, GUOQIANG LI, MING JIN, HAIXIA ZHANG, XIAOYAN WANG, CHRISTOPHER OLDKNOW, ZHONG WANG and XIN HUANG

Key Laboratory of Western China's Environmental Systems (Ministry of Education), College of Earth and Environmental Sciences, Lanzhou University, Lanzhou 730000, China

Received 28 December 2018

Accepted 2 March 2020

Abstract: The residual ages and bleaching of K-feldspar post-IR IRSL (pIRIR) signals (pIR₅₀IR₁₇₀, pIR₅₀IR₂₉₀, and pIR₂₀₀IR₂₉₀) for a variety of modern sediment sources to the Bosten Lake basin in the southern Tian Shan of arid central Asia were assessed to identify the most appropriate facies to sample for ascertaining well-bleached, depositional ages associated with Quaternary paleolake development. Results indicate pIR₅₀IR₂₉₀ residual ages for pluvial fan, fluvial, and eolian sediments cluster at 40–6, 6–3, and 2–1 ka, respectively, and are depositional ages. Residual ages of pIR₂₀₀IR₂₉₀ signals are twice that of pIR₅₀IR₂₉₀ signals, while residual ages of pIR₅₀IR₁₇₀ signals are similar to that of pIR₅₀IR₂₉₀ signals for all samples. Eolian and fluvial samples show well-bleached, coarse-grained (90–125 μm) K-feldspar and poorly-bleached coarse grained K-feldspar from pluvial samples. High residual doses in fluvial and pluvial samples indicate it may not be advisable to apply pIRIR dating utilising different pIRIR signals to Holocene lacustrine samples. However, the residual ages measured for eolian deposits are small and can allow precise and robust assessment of paleolake development by targeting the K-feldspar pIR₅₀IR₁₇₀ signal to date Holocene samples and the pIR₂₀₀IR₂₉₀ and pIR₅₀IR₂₉₀ signals to date Pleistocene samples.

Keywords: modern samples, pIRIR, Bosten Lake, residual dose.

1. INTRODUCTION

Luminescence dating has been widely used to date late Quaternary deposits from different geographical areas of the world (Aitken, 1998). Traditionally, optically

stimulated luminescence (OSL) dating of sedimentary quartz has been employed to date sediments from a range of depositional settings (Murray and Wintle, 2000). However, the quartz OSL signal generally saturates between ~100 and 200 Gy, corresponding to 40–80 ka (for a dose rate of 2.5 Gy/ka) (Wintle, 2008) but is also insensitive in some regions of the world (Preusser *et al.*, 2006; Fuchs *et al.*, 2012; Rhodes, 2015, Li *et al.*, 2018). The recent development of post-IR IRSL (pIRIR) methods applied to K-rich feldspar isolates a slower or completely

Corresponding author: G. Li
e-mail: gqli@lzu.edu.cn

non-faded IRSL signal capable of dating sediments up to 250–300 ka owing to the higher saturation dose of K-feldspar relative to quartz (Thomsen *et al.*, 2008; Buylaert *et al.*, 2012). pIRIR methods have been particularly successful for dating well-bleached eolian deposits like loess and dunes (Buylaert *et al.*, 2012; Yi *et al.*, 2016; Li *et al.*, 2017). However, K-feldspar pIRIR bleaches more slowly relative to quartz particularly at higher stimulation temperatures (e.g., 225–290°C) which may result in age overestimation for samples from depositional environments (e.g. fluvial, glaciofluvial) where signal resetting is not easily achieved (Lawson *et al.*, 2012; Smedley *et al.*, 2015; Colarossi *et al.*, 2015). In fluvial settings, high-energy conditions of transport, or transport of sediment in deep water may occlude grains from receiving equal sunlight exposure resulting in age overestimation (Murray *et al.*, 1995; Olley *et al.*, 1998; 1999; Stokes *et al.*, 2001; Buylaert *et al.*, 2013). Though a number of studies have demonstrated low residual doses for fluvial and coastal samples (Godfrey-Smith *et al.*, 1988; Stokes, 1992; Aitken and Xie, 1992), partial bleaching has been frequently observed for alluvial and lacustrine sediments (Mejdahl and Funder, 1994; Trauerstein *et al.*, 2014; McGuire and Rhodes, 2015). A key concern using pIRIR signals from K-feldspar is accurately quantifying the size of the residual dose which has been found to exhibit large variations in part due to bleaching. For modern loess samples collected from different areas of NW China, the residual dose of quartz OSL signal from the fine-grained loess fraction is generally less than 1 Gy. In contrast, the residual doses from the pIR₅₀IR₂₂₅ and pIR₅₀IR₂₉₀ signals of K-feldspar are much higher varying between 2 and 5 Gy, and between 5 and 19 Gy, respectively (Buylaert *et al.*, 2011). Furthermore, long-term laboratory bleaching using a SOL2 solar simulator for K-feldspar samples from the loess-paleosol sequence from NE China shows that the residual dose of pIR₅₀IR₂₉₀ signal reached a constant (or very difficult to bleach) dose of 6.2 ± 0.7 Gy after ~300 h bleaching (Yi *et al.*, 2016). The pIR₅₀IR₂₉₀ residual doses of modern samples from a glaciated bay at NW Svalbard ranged from 20 to 50 Gy (Alexanderson and Murray 2012; Murray *et al.*, 2012), while the K-feldspar pIR₅₀IR₂₉₀ residual doses from fluvial sediments from different geographical locations ranged from 5 and 10 Gy (Murray *et al.*, 2012). In addition, the residual doses of pIR₅₀IR₂₂₅, pIR₅₀IR₂₉₀ and pIR₂₀₀IR₂₉₀ and MET-pIRIR signals of well-bleached and poorly-bleached samples were measured by the Chen *et al.* (2013). Their results indicate that the poorly-bleached samples have larger residual dose than well-bleached samples and thus the residual dose values might be used to check the resetting of samples before burial (Chen *et al.*, 2013).

Lacustrine sediments are conventionally dated using radiocarbon methods, but this is not always possible particularly in previously glaciated settings where there may be contaminated by old carbon (Dodson and Zhou, 2000; Pessenda *et al.*, 2001; Long and Shen, 2015; Long

and Zhang, 2016). In addition, the upper limit of ¹⁴C dating may be lower than theoretical values due to the low organic content in arid regions (Long and Zhang, 2016). Recently, quartz OSL dating has been successfully applied in the arid regions in China to develop chronologies of lacustrine sedimentation (Chen *et al.*, 2008; Madsen *et al.*, 2008; Li *et al.*, 2015a; Long *et al.*, 2015; Zhang *et al.*, 2016). The tendency of the quartz OSL signal to saturate at less than 60 ka in many parts of China (Buylaert *et al.*, 2007; Chapot *et al.*, 2012; Li *et al.*, 2014; Song *et al.*, 2018) is currently a major obstruction to developing extended chronologies in a range of lacustrine contexts.

As an alternative, dating of lacustrine sediments using pIRIR methods could be facilitated by selecting profiles containing sediments which were subjected to transport conditions optimal for inducing signal resetting. Important developments to the pIRIR protocol (Buylaert *et al.*, 2011) include stimulations at lower temperatures (*i.e.* the pIR₅₀IR₁₇₀) which has the advantage of accessing a more easily “bleachable” signal (Li *et al.*, 2015b). However, a comparative study of different pIRIR signals in lacustrine contexts has yet to be undertaken.

Bosten Lake, located in the central Tian Shan, arid Central Asia (ACA), is the second-largest freshwater lake in China. In this study, different potential sources of sediments in the Bosten Lake Basin were collected to evaluate the bleachability of different pIRIR signals (e.g. pIR₅₀IR₁₇₀, pIR₅₀IR₂₉₀ and pIR₂₀₀IR₂₉₀). The collected samples include: (i) three samples from pluvial fans deposited along the northern margin of the lake; (ii) six samples from point bars at different locations along the Kaidu River; (iii) four eolian sand samples from dunes around Bosten Lake (Fig. 1b). The residual doses of different pIRIR signals (pIR₅₀IR₁₇₀, pIR₅₀IR₂₉₀ and pIR₂₀₀IR₂₉₀) were measured, and the degree to which they are bleached was evaluated. The extent of signal resetting of different catchment sediments of lake sediment and the suitability of each K-feldspar pIRIR signal as a chronometer of lake sediment deposition is discussed.

2. GEOGRAPHICAL SETTING

Bosten Lake (41°56′–42°14′N, 86°40′–87°26′E) is located on the southeastern side of the Yanqi basin on the southern slope of the Tian Shan, NW China, which is the second-largest inland freshwater lake in China. The Yanqi basin is 56,000 km² (Cheng, 1993) and is flanked by the northern Tian Shan in the north and Horo-Kurnktag Mountains in the south (Fig. 1a). Bosten Lake extends 25 km from north to south and 55 km from west to east covering an area of ~1000 km². The average depth of the lake is 10 m, with a maximum depth of 17 m (Xiao *et al.*, 2010). Bosten Lake is fed by 13 rivers, the largest of which is the Kaidu River, which supplies at least 85% of the total surface runoff in the whole basin (Wünnemann *et al.*, 2006). The Konqi River flows out of Bosten Lake

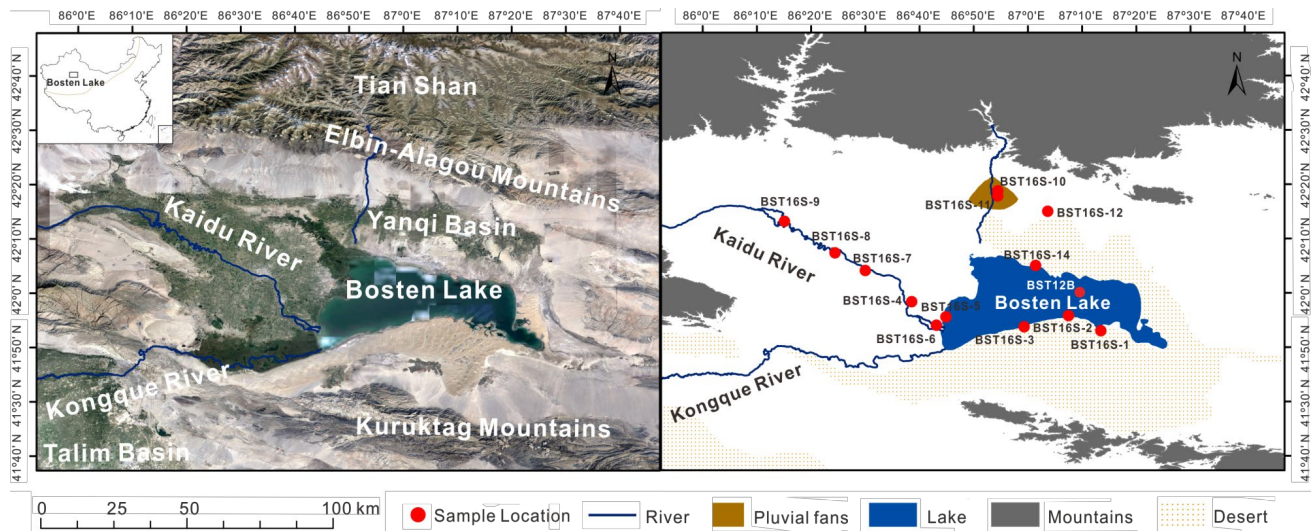


Fig. 1. a) location map indicating position of Bosten Lake located on the southeastern side of the Yanqi basin on the southern slope of the Tian Shan Mountain; b) indicates the distribution of different modern depositional environments around the Bosten Lake Basin which were sampled. Four eolian sand samples (BST16S-1, BST16S-2, BST16S-3, and BST16S-14) were collected from the widespread sand dune field around the lake. Six samples BST16S-4, BST16S-5, BST16S-6, BST16S-7, BST16S-8 and BST16S-9 were collected from the over flooding deposit at different points of Kaidu River channel. Three samples BST16S-10, BST16S-11 and BST16S-12 were collected from the surface of the pluvial fan down the Elbin-Alagou Mountains. The red circle with BST12B besides is the location of drill core BST12B from Li *et al.* (2016).

into the Tarim Basin (Wünnemann *et al.*, 2006). The Yanqi Basin is climatically dominated by the Westerlies. Annual precipitation in Bosten lake basin is 68.2 mm which mainly falls in the summer. The mean annual temperature is 6.3°C (Liu *et al.*, 2013). The annual average evaporation is about 2000 mm (Xu *et al.*, 1996). From high to low altitude, there are five distinct zones of regional vegetation: 1) the Alpine cushion vegetation zone at 3800–3500 m a.s.l.; 2) the alpine meadow zone (3500–2800 m a.s.l.); 3) the grassland belt (2800–2100 m); 4) desert steppe zone (2100–1600 m a.s.l.), dominated by *Neopallasia pestinata* and *Artemisia macrocephala*; 5) the desert zone below 1600 m a.s.l. consisting of desert vegetation growing on the piedmont pluvial fans (Huang *et al.*, 2004).

3. MATERIALS AND METHODS

Sampling

The potential source materials of lake sediment from Bosten Lake mainly consist of fluvial sediments transported by the Kaidu River, and aeolian sand dunes and pluvial fans deposited around the lake. A total of thirteen modern samples were collected from different locations of the lake basin (Fig. 1b, Table 1). The locations of modern analogue samples collected from different potential sources of lake sediment at Bosten Lake Basin are shown in Fig. 2. Samples were collected from 5 cm below the surface of these deposits and were sealed in black bags to avoid light exposure and evaporation of moisture during transportation.

Table 1. The location and sediment type of samples from Bosten lake Basin.

Sample No.	Source material	Distance from Lake (km)	Site	Altitude (m)
BST16S-1	Eolian sand dunes	Around 0.05 km	41.88N, 87.22E	1061
BST16S-2	Eolian sand dunes	Around 0.07 km	41.93N, 87.13E	1060
BST16S-3	Eolian sand dunes	Around 0.10 km	41.90N, 86.99E	1055
BST16S-14	Eolian sand dunes	Around 0.19 km	42.08N, 87.02E	1056
BST16S-4	Fluvial sand from Kaidu river	Around 16.29 km	41.97N, 86.64E	1055
BST16S-5	Fluvial sand from Kaidu river	0	41.93N, 86.75E	1051
BST16S-6	Fluvial sand from Kaidu river	Around 3.33 km	41.90N, 86.72E	1050
BST16S-7	Fluvial sand from Kaidu river	Around 36.14 km	42.07N, 86.50E	1061
BST16S-8	Fluvial sand from Kaidu river	Around 48.54 km	42.12N, 86.41E	1067
BST16S-9	Fluvial sand from Kaidu river	Around 78.92 km	42.22N, 86.25E	1078
BST16S-10	Gravel sand from pluvial fans	Around 21.72 km	42.31N, 86.91E	1166
BST16S-11	Gravel sand from pluvial fans	Around 20.45 km	42.30N, 86.91E	1140
BST16S-12	Gravel sand from pluvial fans	Around 19.59 km	42.25N, 87.06E	1114



Fig. 2. Locations of modern analogue samples collected from different potential sources of lake sediment at Bosten Lake Basin.

Luminescence dating samples preparation and measurement

Sample pretreatments and luminescence measurements were conducted in a darkroom under subdued red light. Sample preparation followed the methods described by Aitken (1998). The preparation method comprises the following steps: firstly, soaking the samples in HCl (10%) and H₂O₂ (30%) for removal of CaCO₃ and organic matter, respectively. Samples were then wet sieved to obtain the 90–125 µm fraction, from which K-rich feldspar was concentrated using sodium polytungstate liquid at a density of 2.58 g/cm³. The K-feldspar fraction was etched using 10% HF for 40 min to remove the outer layer irradiated by alpha particles. Finally, the samples were dissolved by using 1 mol/L HCl for 15 min to remove fluorides created during the HF etching. A total of thirteen K-feldspar samples were prepared for measure-

ment. Etched grains were mounted on 5–6 mm aliquots using silkospray.

Luminescence signals were measured using an automated Risø TL/OSL-DA-20 reader (Bøtter-Jensen *et al.*, 2003) equipped with blue LEDs (470 nm, ~80 Mw/cm²) and IR LEDs (870 nm, ~135 mWcm⁻²). Laboratory irradiation was conducted by using ⁹⁰Sr/⁹⁰Y sources mounted on the reader. The IRSL signal was observed using a PMT with the IRSL passing through Schott BG-39 and Corning 7–59 filters. Sample equivalent doses (D_e) and residual doses were measured using the pIRIR protocol at different elevated temperatures (pIR₅₀IR₂₉₀, pIR₂₀₀IR₂₉₀ and pIR₅₀IR₁₇₀ signals) (Table 2). Test dose size was set to 30% or more of sample D_e for sensitivity correction (Yi *et al.*, 2016). In order to reduce the influence of temperature on the recuperation of the young samples, a 200 s stimulation using the IR LED array was conducted at

Table 2. The pIRIR dating protocol using: (i) the pIR₅₀IR₁₇₀ signal (Li *et al.*, 2015b); (ii) the pIR₅₀IR₂₉₀ signal (Thiel *et al.*, 2011); and (iii) the pIR₂₀₀IR₂₉₀ signal (Li and Li, 2012).

Step	pIR ₅₀ IR ₁₇₀ dating protocol	Observed	pIR ₅₀ IR ₂₉₀ dating protocol	Observed	pIR ₂₀₀ IR ₂₉₀ dating protocol	Observed
1	Give dose D_j^a		Give dose D_j^a		Give dose D_j^a	
2	Preheat at 200°C for 60 s		Preheat at 320°C for 60 s		Preheat at 320°C for 60 s	
3	IRSL, 200 s at 50°C	L_{x1}	IRSL, 200 s at 50°C	L_{x1}	IRSL, 200 s at 200°C	L_{x1}
4	pIRIR, 200 s at 170°C	L_{x2}	pIRIR, 200 s at 290°C	L_{x2}	pIRIR, 200 s at 290°C	L_{x2}
5	Give test dose		Give test dose		Give test dose	
6	Preheat at 200°C for 60 s		Preheat at 320°C for 60 s		Preheat at 320°C for 60 s	
7	IRSL, 200 s at 50°C	T_{x1}	IRSL, 200 s at 50°C	T_{x1}	IRSL, 200 s at 200°C	T_{x1}
8	pIRIR, 200 s at 170°C	T_{x2}	pIRIR, 200 s at 290°C	T_{x2}	pIRIR, 200 s at 290°C	T_{x2}
9			IRSL, 200s bleaching at 325°C		IRSL, 200s bleaching at 325°C	
10	Return to 1		Return to 1		Return to 1	

325°C at the end of each single aliquot regenerative (SAR) cycle (Jain and Ankjærgaard, 2011; Buylaert *et al.*, 2015).

Dose recovery tests for the different pIRIR signals were conducted on sample BST16S-1 to check the suitability of the SAR protocol for the modern samples (Wallinga *et al.*, 2000). For each pIRIR SAR protocol, two given doses of 22.63 Gy and 188.60 Gy were added to two groups of the sample (4 aliquots each group), respectively, and then the dose was measured as an unknown dose using the protocol shown in Table 2. Sample D_e was then calculated for each of the three pIRIR protocols (Table 3).

In order to check the bleachability of the pIRIR signals of samples from the Bosten lake area, all K-feldspar samples (three aliquots each sample) were exposed to sunlight for 112 h (8 h per day, 2 weeks, April, 2018, Lanzhou, China), and then the residual doses were measured using the three pIRIR dating protocols (Table 2).

The dose rate of all samples was obtained by measuring the radioactive element concentrations of uranium (U) and thorium (Th) and potassium (K) content using Neutron Activation Analysis. For each sample, ~5 g of each sample was ground to < 4 µm using an agate mortar. All results were converted to beta and gamma dose rates according to the conversion factors of Guérin *et al.* (2011). As listed in Table 3, the measured water content (% by dry weight) of eolian sand samples from Bosten Lake (BST16S-1, BST16S-2, BST16S-3 and BST16S-14) ranges from 0.03% to 0.3%. The observed water content of fluvial samples collected from Bosten lake (BST16S-4, BST16S-7, BST16S-8 and BST16S-9) range from 1% to 9%, except samples BST16S-5, BST16S-6 (25 and 32% water content) which were collected from subaqueous contexts (river delta and river channel, respectively). The observed water content of samples collected from pluvial fans from Bosten Lake (BST16S-10, BST16S-11 and BST16S-12) ranges from 0.2% to 2%. As a result, the life average water content of $1 \pm 0.5\%$, $6 \pm 3\%$ and $1 \pm 0.5\%$ are used for eolian sand, fluvial and pluvial samples, respectively given the uncertainty of samples after deposition. The cosmic dose rate was calculated according to the altitudes of sample location and burial depth (Prescott and Hutton, 1994). The internal dose rate of K-feldspar grains was calculated assuming a K content of $12.5 \pm 0.5\%$ (Huntley and Baril, 1997) and Rb content of 400 ± 100 ppm (Huntley and Hancock, 2001; Zhao and Li, 2005).

4. RESULTS AND DISCUSSION

Luminescence characteristics of K-feldspar pIRIR signals of samples from Bosten Lake Basin

The dose recovery test results of sample BST16S-1 for pIR₅₀IR₁₇₀, pIR₅₀IR₂₉₀ and pIR₂₀₀IR₂₉₀ signals are illustrated in Fig. 3. The calculated measured/given (M/G here in) dose ratio all lie within 10% of unity except for

pIR₅₀IR₂₉₀ signal for the large given dose of 188.60 Gy. The recycling ratio of all measurement for pIRIR signals fall in 0.98–1.02 and the recuperation of the natural signal for all aliquots is less than ~4%. These data indicate that the pIRIR dating protocols using pIR₅₀IR₁₇₀, pIR₅₀IR₂₉₀ and pIR₂₀₀IR₂₉₀ signals can be used to measure the D_e of these samples from Bosten Lake Basin.

The growth curve and decay curves of pIR₅₀IR₁₇₀, pIR₅₀IR₂₉₀, and pIR₂₀₀IR₂₉₀ signals for a K-feldspar sample (BST16S-5) are illustrated in Fig. 4. The natural pIR₅₀IR₁₇₀, pIR₅₀IR₂₉₀, and pIR₂₀₀IR₂₉₀ signals of the sample are bright enough for D_e determination. The growth curves for the pIR₅₀IR₁₇₀, pIR₅₀IR₂₉₀ and pIR₂₀₀IR₂₉₀ signals of all samples were fitted using a single exponential function.

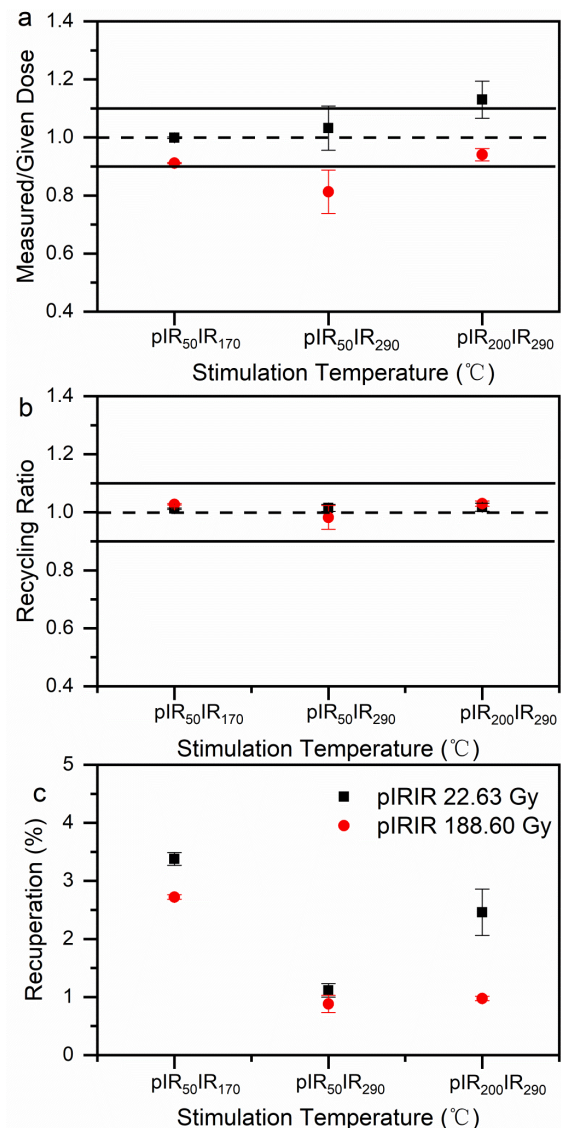
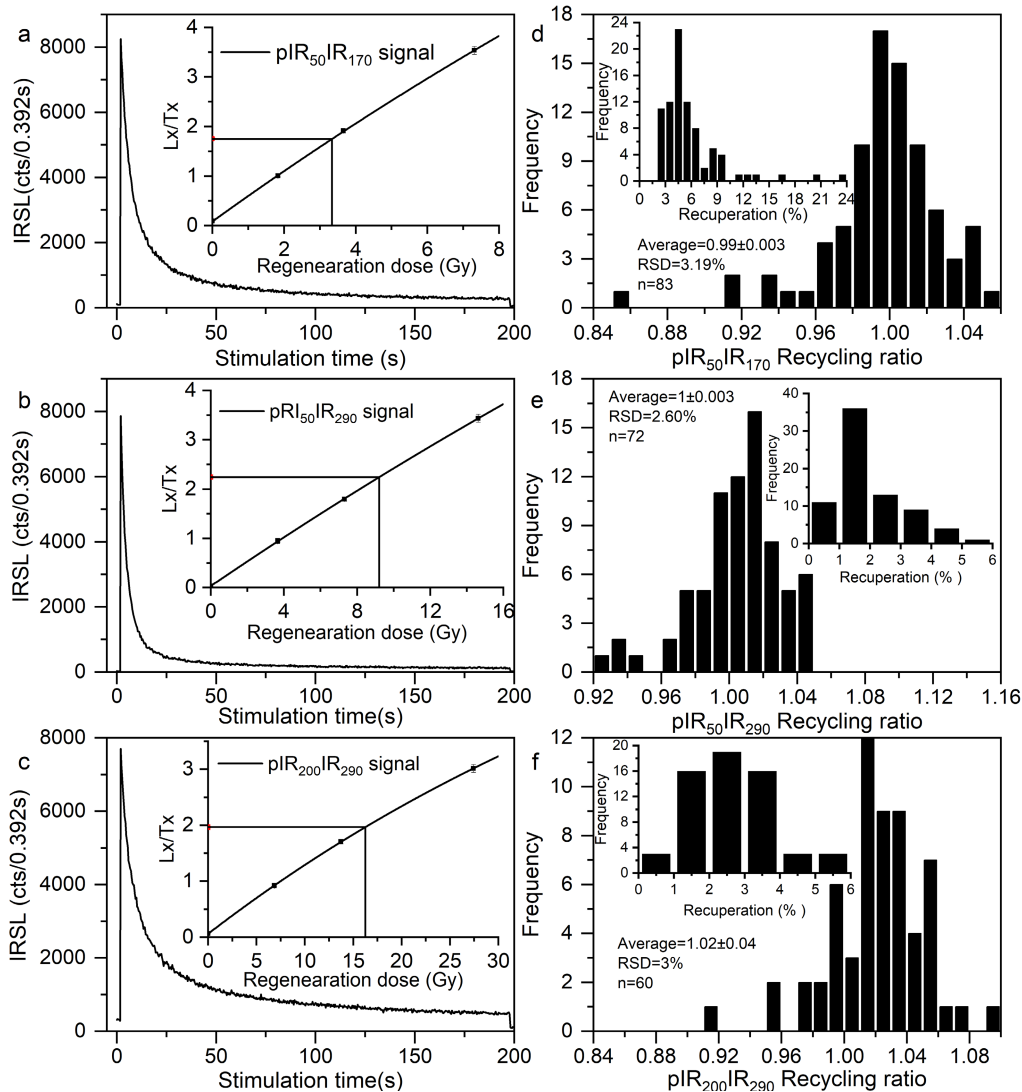


Fig. 3. a) b) c) show the dose recovery test results from sample BST16S-1. a is the measured dose/given (M/G) dose; b) and c) show the recycling ratios and recuperation values.

Table 3. Dose rate data based on Neutron Activation Analysis for samples from Bosten lake Basin.

Sample No.	Grain size (μm)	U (ppm)	Th (ppm)	K (%)	Observed water content (%)	Life average water content (%)	Internal dose rate (Gy/ka)	Cosmic dose rate (Gy/ka)	Dose rate (Gy/ka)
BST16S-1	90–125	1.58 ± 0.07	4.9 ± 0.17	1.67 ± 0.06	0.20	1 ± 0.5	0.46 ± 0.03	0.33	3.21 ± 0.06
BST16S-2	90–125	1.08 ± 0.06	3.74 ± 0.14	2.29 ± 0.07	0.40	1 ± 0.5	0.46 ± 0.03	0.33	3.66 ± 0.06
BST16S-3	90–125	1.27 ± 0.06	5.18 ± 0.18	1.99 ± 0.06	0.05	1 ± 0.5	0.46 ± 0.03	0.33	3.50 ± 0.06
BST16S-14	90–125	1.44 ± 0.07	5.33 ± 0.18	1.62 ± 0.05	0.03	1 ± 0.5	0.46 ± 0.03	0.33	3.16 ± 0.06
BST16S-4	90–125	2.33 ± 0.09	11.8 ± 0.33	1.79 ± 0.06	4.5	6 ± 3	0.46 ± 0.03	0.33	3.83 ± 0.12
BST16S-5	90–125	1.33 ± 0.07	6.07 ± 0.20	1.94 ± 0.06	24.8	6 ± 3	0.46 ± 0.03	0.33	3.37 ± 0.10
BST16S-6	90–125	1.71 ± 0.08	6.33 ± 0.21	2.03 ± 0.06	32.5	6 ± 3	0.46 ± 0.03	0.33	3.72 ± 0.12
BST16S-7	90–125	1.74 ± 0.08	7.26 ± 0.23	2.13 ± 0.06	1.2	6 ± 3	0.46 ± 0.03	0.33	3.72 ± 0.11
BST16S-8	90–125	1.67 ± 0.08	8.56 ± 0.26	2.09 ± 0.06	2.7	6 ± 3	0.46 ± 0.03	0.33	3.76 ± 0.12
BST16S-9	90–125	1.84 ± 0.08	8.59 ± 0.26	2.13 ± 0.06	8.6	6 ± 3	0.46 ± 0.03	0.33	3.84 ± 0.12
BST16S-10	90–125	2.36 ± 0.09	12.9 ± 0.36	2.05 ± 0.06	2.1	1 ± 0.5	0.46 ± 0.03	0.34	4.37 ± 0.07
BST16S-11	90–125	1.86 ± 0.08	9.82 ± 0.28	2.32 ± 0.07	2.2	1 ± 0.5	0.46 ± 0.03	0.33	4.32 ± 0.07
BST16S-12	90–125	1.97 ± 0.08	12.6 ± 0.35	2.54 ± 0.07	0.2	1 ± 0.5	0.46 ± 0.03	0.33	4.77 ± 0.07

**Fig. 4.** Luminescence characteristics of K-feldspar pIRIR signal for samples: a), b) and c) show representative decay and growth curves from the pIR₅₀IR₁₇₀, IR₅₀, pIR₅₀IR₂₉₀, IR₅₀ and pIR₂₀₀IR₂₉₀, IR₂₀₀ signals for K-feldspar sample BST16S-5. d), e) and f) show the recycling ratios and recuperation values of all aliquots for the pIR₅₀IR₁₇₀, pIR₅₀IR₂₉₀ and pIR₂₀₀IR₂₉₀ D_e measurements for all samples, respectively.

For the $pIR_{50}IR_{170}$ D_e measurements, the average recycling ratio for all 83 aliquots of the 13 K-feldspar samples is 0.99 ± 0.003 . The recuperation of the signals for almost all aliquots (77) is less than 10%, except for six aliquots (Fig. 4d). For the $pIR_{50}IR_{290}$ and $pIR_{200}IR_{290}$ D_e measurement, the average recycling ratio of the 13 K-feldspar samples is within 10% of unity. The recuperation of the natural signals for more than 95% aliquots is less than 5% (Fig. 4e and 4f). Together these results indicate the pIRIR D_e measurements are acceptable. The average value of 4–14 aliquots' D_e was used to calculate the pIRIR D_e for each K-feldspar sample. The calculated K-feldspar IR and pIRIR D_e s, and ages for all samples are listed in Table 4.

The pIRIR residual doses from different source materials

K-feldspar pIRIR residual D_e s for samples from different sources exhibit large differences (Fig. 5). For all samples, the measured D_e values show a well-ordered increase with stimulation temperature irrespective of source, which shows that the bleach rates of the lower

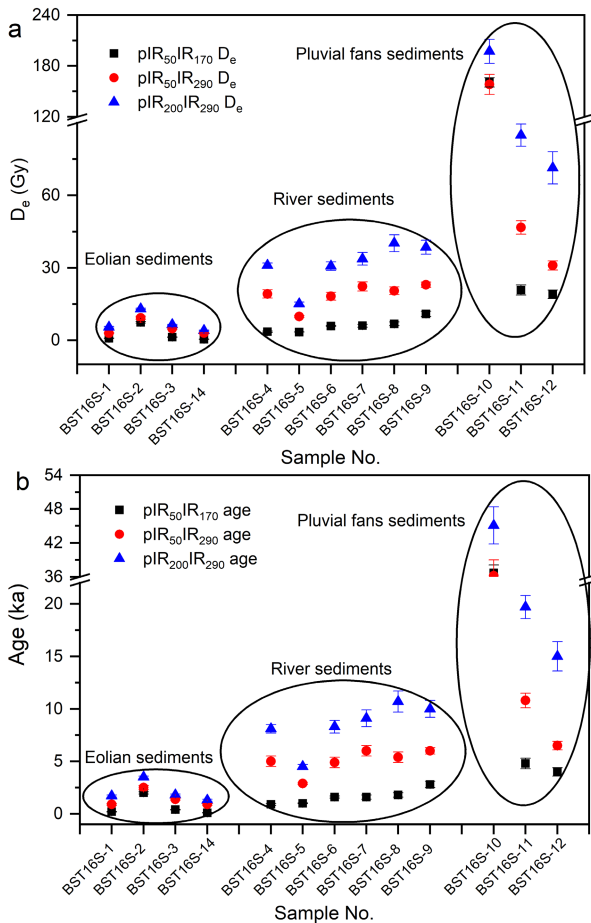


Fig. 5. The distribution of D_e (a) and age (b) values obtained using different pIRIR signals ($pIR_{50}IR_{170}$ D_e , $pIR_{50}IR_{290}$ D_e and $pIR_{200}IR_{290}$).

Table 4. Summary of K-feldspar pIRIR age data for samples from Bosten lake Basin.

Sample No.	$pIR_{50}IR_{170}$ D_e (Gy)	$pIR_{50}IR_{290}$ D_e (Gy)	$pIR_{200}IR_{290}$ D_e (Gy)	IR ₅₀ D_e (Gy)	IR ₂₀₀ D_e (Gy)	IR _{50} D_e (Gy)}	IR ₂₀₀ D_e (Gy)	$pIR_{50}IR_{170}$ D_e (Gy)	$pIR_{50}IR_{290}$ D_e (Gy)	$pIR_{200}IR_{290}$ D_e (Gy)	OD (%)	OD (%)	OD (%)	IR ₅₀ Age (ka)	IR ₂₀₀ Age (ka)	$pIR_{50}IR_{290}$ Age (ka)	$pIR_{200}IR_{290}$ Age (ka)	
BST16S-1	11/5/4	0.8±0.3	0.8±0.1	0.3±0.03	2.9±0.2	1.8±0.2	1.8±0.2	2.9±0.2	2.9±0.2	5.4±0.3	72±15	11±4	9±4	0.2±0.1	0.2±0.03	0.1±0.01	0.9±0.1	1.7±0.1
BST16S-2	4/8/4	4.6±0.1	7.4±0.3	3.3±0.3	9.3±0.7	5.1±0.6	5.1±0.6	9.3±0.7	9.3±0.7	13.0±0.3	5±2	23±6	4±2	1.3±0.04	2.0±0.1	0.9±0.1	2.5±0.2	3.5±0.1
BST16S-3	4/5/4	0.6±0.04	1.3±0.1	0.9±0.1	4.8±0.4	1.8±0.1	1.8±0.1	4.8±0.4	4.8±0.4	6.4±0.2	9±3	15±5	3±2	0.2±0.01	0.4±0.03	0.3±0.03	1.4±0.1	1.8±0.1
BST16S-14	11/5/4	0.2±0.1	0.4±0.1	0.4±0.1	3.0±0.2	1.0±0.02	1.0±0.02	3.0±0.2	3.0±0.2	4.0±0.2	53±11	12±4	7±3	0.1±0.03	0.1±0.03	0.1±0.03	0.9±0.1	1.3±0.1
BST16S-4	4/4/4	0.8±0.1	3.5±0.3	3.1±0.5	19.2±1.7	6.5±0.2	31.0±1.0	19.2±1.7	31.0±1.0	31.0±1.0	16±6	16±6	4±2	0.2±0.03	0.9±0.1	0.8±0.1	5.0±0.5	8.1±0.4
BST16S-5	4/4/5	1.2±0.1	3.4±0.04	1.6±0.2	9.8±0.2	3.9±0.3	15.1±0.7	9.8±0.2	15.1±0.7	15.1±0.7	0	7±3	7±3	0.4±0.03	1.0±0.03	0.5±0.1	1.2±0.1	4.5±0.2
BST16S-6	4/4/6	1.7±0.1	5.9±0.2	3.2±0.3	18.2±1.6	7.5±0.4	30.7±1.8	18.2±1.6	30.7±1.8	30.7±1.8	5±2	16±6	10±4	0.5±0.03	1.6±0.1	0.9±0.1	2.9±0.1	8.3±0.6
BST16S-7	8/4/4	1.8±0.1	6.0±0.6	2.9±0.1	22.3±1.9	7.9±1.0	33.7±2.6	22.3±1.9	33.7±2.6	33.7±2.6	24±6	15±6	13±5	0.5±0.03	1.6±0.2	0.8±0.04	6.0±0.5	2.1±0.3
BST16S-8	8/7/8	2.7±0.9	6.8±0.8	2.9±0.3	20.5±1.6	8.9±1.1	40.2±3.5	20.5±1.6	40.2±3.5	40.2±3.5	32±8	22±6	19±5	0.7±0.2	1.8±0.2	0.8±0.1	5.4±0.5	2.4±0.3
BST16S-9	8/7/9	2.2±0.2	10.9±1.1	4.1±0.6	23.0±1.1	10.2±0.8	38.5±2.9	23.0±1.1	38.5±2.9	38.5±2.9	31±8	14±4	21±5	0.6±0.1	2.8±0.3	1.1±0.2	6.0±0.3	2.7±0.2
BST16S-10	8/5/4	89.0±3.8	160.5±5.5	60.5±5.7	158.2±11.8	86.6±4.1	197.2±14.1	158.2±11.8	197.2±14.1	197.2±14.1	8±2	15±5	11±4	20.4±0.9	36.7±1.4	13.8±1.3	36.2±2.8	19.8±1
BST16S-11	4/9/4	3.7±0.2	20.8±2.1	7.6±0.5	46.7±2.8	19.8±1.8	84.9±4.6	46.7±2.8	84.9±4.6	84.9±4.6	17±6	18±4	9±3	0.9±0.05	4.8±0.5	1.8±0.1	10.8±0.7	4.6±0.4
BST16S-12	4/5/4	2.2±0.2	19.0±1.8	4.1±0.7	31.0±1.9	18.3±1.8	71.4±6.7	31.0±1.9	71.4±6.7	71.4±6.7	17±6	11±4	16±6	0.5±0.04	4.0±0.4	0.9±0.1	6.5±0.4	3.8±0.4

temperature pIRIR signal is quicker. However, largest residual doses were observed from the pluvial fan samples (19–197 Gy), followed by Kaidu River alluvium (3–40 Gy) and the sand dunes (0.4–13 Gy). Smedley *et al.* (2015) demonstrated that the bleaching rate of pIRIR signal was higher at lower pIRIR stimulation temperature by comparison of pIRIR₂₂₅ and pIRIR₂₉₀ ages of a naturally-bleached dune sand from Argentina using single-grain measurements of the pIRIR₂₂₅ and pIRIR₂₉₀ signals.

The average pIR₅₀IR₁₇₀, pIR₅₀IR₂₉₀ and pIR₂₀₀IR₂₉₀ ages for eolian sand samples are ~ 0.7 ka, 1.5 ka and 2.5 ka, respectively (Fig. 6a). The residual dose from the pIR₅₀IR₁₇₀ signal is negligible as a proportion of age for Holocene samples. The pIR₅₀IR₂₉₀ and pIR₂₀₀IR₂₉₀ signals produce residual doses small enough to justify their application to Pleistocene samples. Thus the coarse-grained K-feldspar transported from dunes around the lake is resetting well and can be used for lake sediment age determination. The average pIR₅₀IR₁₇₀, pIR₅₀IR₂₉₀ and pIR₂₀₀IR₂₉₀ ages of the fluvial samples are ~1.6 ka, 5.1 ka and 8.4 ka, respectively (Fig. 6b). The residual ages of both eolian and fluvial samples exhibit a decreasing trend with proximity to the lake.

Notably, the pIRIR residual ages of the fluvial samples decrease with proximity to the lake (from 4–1 ka) indicating improved bleaching with transport distance (Murray *et al.*, 1995; Stokes *et al.*, 2001; McGuire and Rhodes, 2015). The smallest age of pIRIR₁₇₀ signal for

fluvial samples is ~1 ka, which is acceptably low for dating mid- or early Holocene samples. The ages obtained from the pIR₅₀IR₂₉₀ and pIR₂₀₀IR₂₉₀ signals for fluvial sample are 3 ka and 4 ka, respectively, which indicates they may still be suitable for dating Pleistocene samples.

The hard-to-bleach pIRIR residual dose for samples from different sources in Bosten Lake

The residual doses of pIR₅₀IR₁₇₀, pIR₅₀IR₂₉₀ and pIR₂₀₀IR₂₉₀ for all samples after 112 h sunlight bleaching during April in Lanzhou, China, are listed in Table 5 and illustrated in Fig. 7. The residual doses generally increase with increasing sample age, which is consistent with

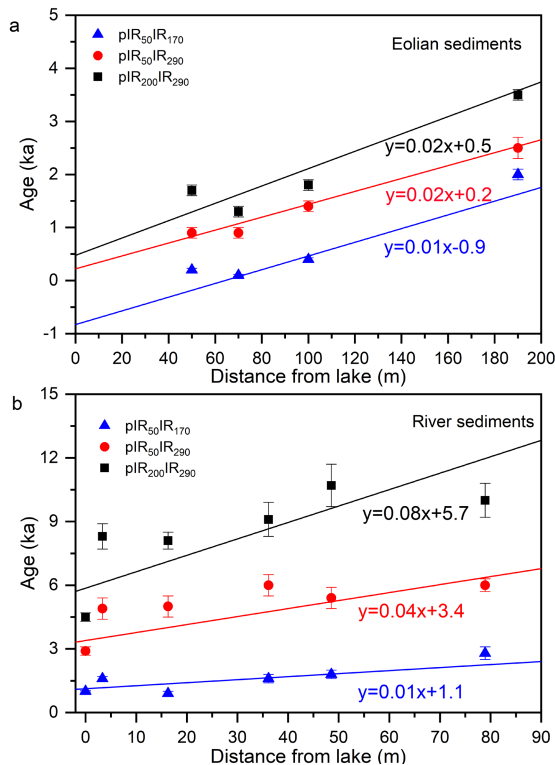


Fig. 6. a) and b) pIRIR ages from eolian and river sediments plotted as a function of distance from sampling sites from Bosten Lake, respectively.

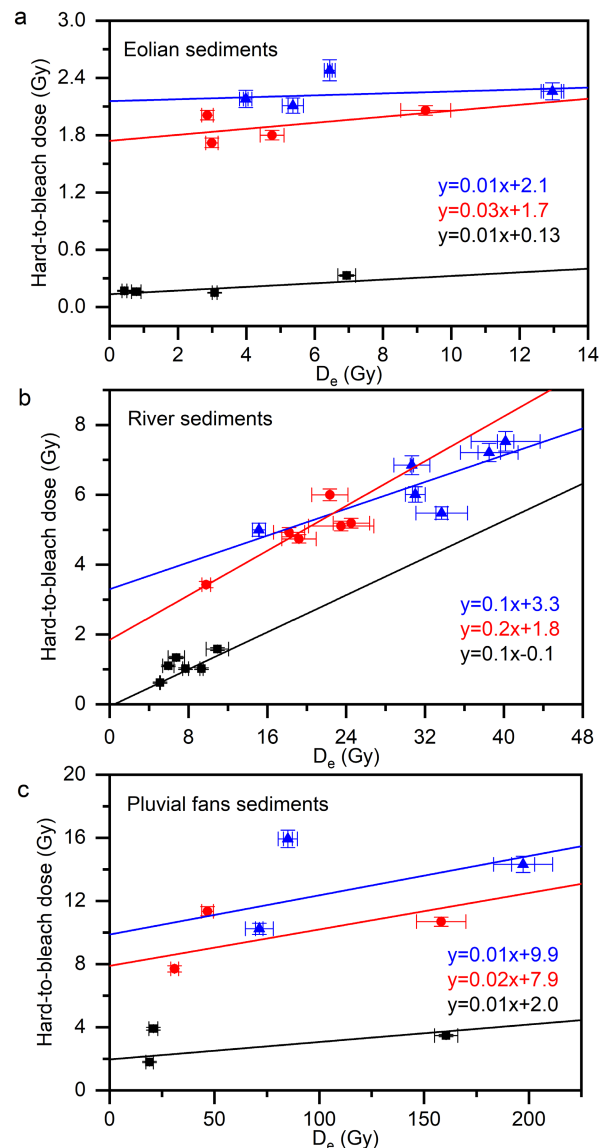


Fig. 7. Plots of the residual doses of eolian samples (a), fluvial samples (b) and pluvial samples (c) obtained using different pIRIR signals after 112 h sunlight bleaching as a function of the associated D_e values.

Table 5. Summary of the residual dose after 112 h bleaching under sunlight for all samples from Bosten lake Basin.

Sample No.	Residual dose (112 h bleaching)					
	IR ₅₀ (Gy)	pIR ₅₀ IR ₁₇₀ (Gy)	IR ₅₀ (Gy)	pIR ₅₀ IR ₂₉₀ (Gy)	IR ₂₀₀ (Gy)	pIR ₂₀₀ IR ₂₉₀ (Gy)
BST16S-1	0.53 ± 0.01	0.10 ± 0.005	0.34 ± 0.01	2.01 ± 0.05	0.76 ± 0.02	2.11 ± 0.08
BST16S-2	0.05 ± 0.001	0.33 ± 0.01	0.32 ± 0.01	2.06 ± 0.05	0.75 ± 0.02	2.26 ± 0.09
BST16S-3	0.07 ± 0.002	0.15 ± 0.005	0.32 ± 0.01	1.80 ± 0.05	0.78 ± 0.02	2.48 ± 0.11
BST16S-4	0.08 ± 0.002	1.02 ± 0.02	0.80 ± 0.02	4.74 ± 0.12	1.82 ± 0.04	6.01 ± 0.22
BST16S-5	0.06 ± 0.002	0.62 ± 0.02	0.65 ± 0.02	3.43 ± 0.09	1.57 ± 0.04	5.00 ± 0.19
BST16S-6	0.39 ± 0.01	1.02 ± 0.02	1.00 ± 0.03	4.93 ± 0.13	1.99 ± 0.04	6.85 ± 0.27
BST16S-7	0.26 ± 0.01	1.10 ± 0.03	0.95 ± 0.02	6.00 ± 0.17	1.66 ± 0.04	5.48 ± 0.18
BST16S-8	0.30 ± 0.01	1.34 ± 0.03	0.89 ± 0.02	5.11 ± 0.14	2.25 ± 0.05	7.53 ± 0.28
BST16S-9	0.42 ± 0.01	1.58 ± 0.04	1.04 ± 0.03	5.19 ± 0.14	2.21 ± 0.05	7.21 ± 0.26
BST16S-10	0.50 ± 0.01	3.47 ± 0.08	1.57 ± 0.04	10.69 ± 0.29	3.50 ± 0.08	14.32 ± 0.51
BST16S-11	0.56 ± 0.01	3.91 ± 0.09	1.77 ± 0.04	11.35 ± 0.29	3.82 ± 0.08	15.94 ± 0.55
BST16S-12	0.89 ± 0.02	1.80 ± 0.04	0.81 ± 0.02	7.70 ± 0.20	3.06 ± 0.07	10.24 ± 0.35
BST16S-14	1.14 ± 0.02	0.17 ± 0.01	0.33 ± 0.01	1.72 ± 0.05	0.80 ± 0.02	2.18 ± 0.09

samples from loess-paleosol sequences in the Tian Shan (Li *et al.*, 2015b). The hard-to-bleach dose component of the residual dose exhibits an increasing trend with stimulation temperature for the same sample.

For eolian samples from dunes around the lake, the hard-to-bleach dose of the pIR₅₀IR₁₇₀ signal ranged from ~0.15 Gy to ~0.33 Gy (~0.03 to ~0.09 ka), which is similar to previously reported hard-to-bleach dose values (< 0.5 Gy) from loess deposited in the Tian Shan (Li *et al.*, 2015b) (Fig. 8a). The hard-to-bleach dose of pIR₅₀IR₂₉₀ and pIR₂₀₀IR₂₉₀ signals for eolian sand samples increased to ~ 2 Gy (~0.6 ka). For the fluvial samples, the hard-to-bleach dose of pIR₅₀IR₁₇₀, pIR₅₀IR₂₉₀ and pIR₂₀₀IR₂₉₀ ranges from 0.6–7.5 Gy (Fig. 8b). For the pluvial fan samples, the hard-to-bleach dose of pIR₅₀IR₁₇₀, pIR₅₀IR₂₉₀ and pIR₂₀₀IR₂₉₀ ranges from 1.8–15.9 Gy (Fig. 8c). These results indicate that the hard-to-bleach dose of pIRIR signal is closely related to the types of source materials. The K-feldspar samples from eolian dunes and fluvial deposit are bleachable and can be reset to a background of 0–0.5 ka using the pIRIR₁₇₀ signal and 1–2 ka using the pIRIR₂₉₀ signal. However, the pluvial fan deposits exhibit anomalously high hard-to-bleach dose values (up to ~18 Gy) when the pIRIR₂₉₀ signal was measured, but this was only ~3 Gy for the pIRIR₁₇₀. These residual dose values cannot be dismissed for the Pleistocene sample when using pIRIR₂₉₀ signal, nor the Holocene samples when using pIRIR₁₇₀ signal. The ages of pIRIR signals of pluvial fan samples vary from 4.0–45.1 ka, which indicates poor bleaching. The hard-to-bleach dose of pIRIR₂₉₀ signal for coarse-grained K-feldspar from a 51.2 m deep lake core from Boston Lake were measured after 112 h sunlight bleaching (Li *et al.*, 2017). As illustrated in Fig. 8d, the hard-to-bleach doses from the pIRIR₂₉₀ signal of the lake sediment range from 2 to 6 Gy, which is much smaller than the pluvial fan deposits (20–50 Gy), is slightly smaller than those obtained (3.8 Gy) from the fluvial deposits but overlaps the values obtained from the eolian dune samples

(1.5–2.5 Gy) (Fig. 8a). These results show that the K-feldspar within the lake sediments was mainly sourced from fluvial and eolian deposits, and the pluvial fans contributed very little sediment. It may not be advisable to apply pIRIR dating utilising different pIRIR signals to Holocene lacustrine samples when the source materials are mainly from pluvial deposits due to their high hard-to-bleach dose. However, the residuals associated with the eolian and fluvial deposit are small enough to warrant dismissal (e.g., Using K-feldspar pIR₅₀IR₁₇₀ signal to date Holocene sample and using pIR₂₀₀IR₂₉₀ and pIR₅₀IR₂₉₀ signals to date Pleistocene samples). When dating water-lain samples, it is advisable to collect samples from areas that exclude inputs from poorly-bleached pluvial fan sediments.

The possibility of distinguishing fluvial and eolian source materials for age determination based on the depositional process of lake sediment is helpful for discussion of the reliability of the chronology. A key advantage of using a low stimulation temperature for pIRIR dating can substantially reduce significant contributions of a residual dose (Kars *et al.*, 2014).

5. CONCLUSION

A series of potential sediment source materials (sand dunes, river sediments and pluvial fan sediments) around Bosten Lake, arid central Asia were sampled to investigate the extent to which different pIRIR signals (pIR₅₀IR₁₇₀, pIR₅₀IR₂₉₀ and pIR₂₀₀IR₂₉₀) had been bleached. There is a significant difference in both the residual and hard-to-bleach doses from the different types of sources materials. When the sampling site is closer to the lake, its pIRIR residual dose is lower. Until the sampling point is located under the lake, the residual ages up to 4.5 ka can be considered well-bleached; but in contrast, the pluvial fan sediment is very poor-bleached. The residual doses of both fluvial and eolian samples were shown to be sensitive to pIRIR stimulation temperature.

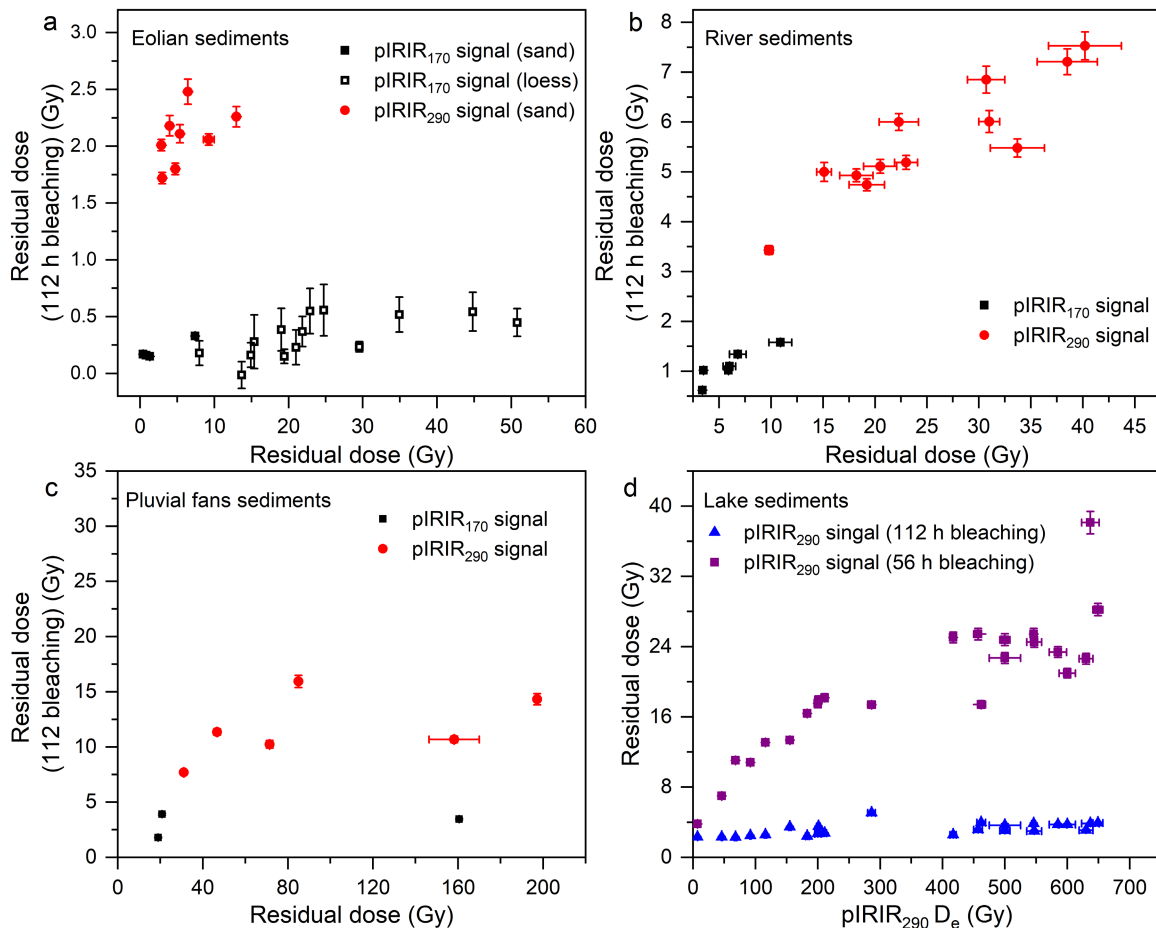


Fig. 8. a), b), c) and d) show the hard-to-bleach dose values for eolian, fluvial, and pluvial and lacustrine samples, respectively. $pIR_{50}IR_{170}$ residual dose of loess (red circles) in a) and $pIR_{50}IR_{290}$ residual dose of lacustrine samples (square and triangle) in d) are cited from Li *et al.* (2015b) and Li *et al.* (2016), respectively.

The evidence in this paper indicates that the $pIR_{50}IR_{170}$ signal is the most suitable for dating Holocene samples, but the $pIR_{200}IR_{290}$ or $pIR_{50}IR_{290}$ signals can be used to date older Pleistocene material at sections containing reworked fluvial or eolian material can be demonstrated. Efforts to date the sediments of Bosten Lake using pIRIR methods should take care to exclude sections likely to have been influenced by significant inputs of poorly bleached pluvial fan material. This study provides an important methodological basis for testing the suitability of pIRIR dating in lacustrine environments and would be an important step forward in constraining the chronology of lacustrine sedimentation, particularly in areas where radiocarbon dating methods are unsuitable.

ACKNOWLEDGMENTS

We thank Dr. Haichao Xie and Zhiping Zhang for their help during fieldwork. This study was supported by the NSFC grant No. 41790423, 41771210 and 41571181.

REFERENCES

- Aitken MJ, 1998. *An Introduction to Optical Dating*. 267 pp. Oxford University Press, Oxford.
- Aitken MJ and Xie J, 1992. Optical dating using infrared diodes: young samples. *Quaternary Science Reviews* 11(1–2): 147–152, DOI 10.1016/0277-3791(92)90056-E.
- Alexanderson H and Murray AS, 2012. Luminescence signals from modern sediments in a glaciated bay, NW Svalbard. *Quaternary Geochronology* 10: 250–256, DOI 10.1016/j.quageo.2012.01.001.
- Bøtter-Jensen L, Andersen CE, Duller GAT and Murray AS, 2003. Developments in radiation, stimulation and observation facilities in luminescence measurements. *Radiation Measurements* 37(4–5): 535–541, DOI 10.1016/S1350-4487(03)00020-9.
- Buylaert JP, Murray AS, Gebhardt AC, Sohbati R, Ohlendorf C, Thiel C, Wastegard S and Zolitschka B, 2013. Luminescence dating of the pasado core 5022-1d from Laguna Potrok Aike (Argentina) using IRSL signals from feldspar. *Quaternary Science Reviews* 71(1): 70–80, DOI 10.1016/j.quascirev.2013.03.018.
- Buylaert JP, Thiel C, Murray AS, Vandenberghe DAG, Yi SW and Lu HY, 2011. IRSL and post-IR IRSL residual doses recorded in modern dust samples from the Chinese loess plateau. *Geochronometria* 38(4): 432–440, DOI 10.2478/s13386-011-0047-0.
- Buylaert JP, Jain M, Murray AS, Thomsen KJ, Thiel C and Sohbati R, 2012. A robust feldspar luminescence dating method for middle

- and late Pleistocene sediments. *Boreas* 41(3): 435–451, DOI 10.1111/j.1502-3885.2012.00248.x.
- Buylaert JP, Vandenberghe D, Murray AS, Huot S, Corte FD and Haute PVD, 2007. Luminescence dating of old (>70 ka) Chinese loess: a comparison of single-aliquot OSL and IRSL techniques. *Quaternary Geochronology* 2(1–4): 9–14, DOI 10.1016/j.quageo.2006.05.028.
- Buylaert JP, Yeo EY, Thiel C, Yi SW, Stevens T, Thompson W, Frechen M, Murray A and Lu HY, 2015. A detailed post-IR IRSL chronology for the last interglacial soil at the Jingbian loess site (northern China). *Quaternary Geochronology* 30(8): 194–199, DOI 10.1016/j.quageo.2015.02.022.
- Chapot MS, Roberts HM, Duller GAT and Lai ZP, 2012. A comparison of natural- and laboratory-generated dose response curves for quartz optically stimulated luminescence signals from Chinese loess. *Radiation Measurements* 47(11–12): 1045–1052, DOI 10.1016/j.radmeas.2012.09.001.
- Chen FH, Fan YX, Madsen DB, Chun X, Zhao H and Yang LP, 2008. Preliminary study on the formation mechanism of the “Jilantai-Hetao” Megalake and the lake evolutionary history in Hetao region. *Quaternary Sciences* 28(5): 866–873.
- Chen YW, Li SH and Li B, 2013. Residual doses and sensitivity change of post IR IRSL signals from potassium feldspar under different bleaching conditions. *Geochronometria* 40(4): 229–238, DOI 10.2478/s13386-013-0128-3.
- Cheng QC, 1993. Mineralization of water quality and utilization of water resources of Bosten Lake. *Arid Land Geography*, 04.
- Colarossi D, Duller GAT, Roberts HM, Tooth S and Lyons R, 2015. Comparison of paired quartz OSL and feldspar post-IR IRSL dose distributions in poorly bleached fluvial sediments from South Africa. *Quaternary Geochronology* 30: 233–238, DOI 10.1016/j.quageo.2015.02.015.
- Dodson JR and Zhou W, 2000. Radiocarbon dates from a Holocene deposit in southwestern Australia. *Radiocarbon* 42(02): 229–234, DOI 10.1017/S0033822200059038.
- Fuchs M, Kreutzer S, Fischer M, Sauer D and R Sørensen, 2012. OSL and IRSL dating of raised beach sand deposits along the southeastern coast of Norway. *Quaternary Geochronology* 10(10): 195–200, DOI 10.1016/j.quageo.2011.11.009.
- Godfrey-Smith DI, Huntley DJ, Chen WH, 1988. Optical dating studies of quartz and feldspar sediment extracts. *Quaternary Science Reviews* 7(3): 373–380, DOI 10.1016/0277-3791(88)90032-7.
- Guérin G, Mercier N and Adamiec G, 2011. Dose-rate conversion factors: update. *Ancient TL* 29: 5–8.
- Huang X, Zhao Y, Cheng B, Chen F and Xu J, 2004. Modern Pollen Analysis of the Surface Sediments from the Bosten Lake, Xinjiang, China. *Journal of Glaciology and Geology* 26(5): 602–609. (In Chinese with English abstract).
- Huntley DJ and Baril MR, 1997. The K content of the K-feldspars being measured in optical dating or in thermoluminescence dating. *Ancient TL* 15: 11–13.
- Huntley DJ and Hancock RGV, 2001. The Rb contents of the K-feldspar grains being measured in optical dating. *Ancient TL* 19: 43–46.
- Jain M and Ankjærgaard C, 2011. Towards a non-fading signal in feldspar: insight into charge transport and tunnelling from time-resolved optically stimulated luminescence. *Radiation Measurements* 46(3): 292–309, DOI 10.1016/j.radmeas.2010.12.004.
- Kars RH, Reimann T, Ankjærgaard C and Wallinga J, 2014. Bleaching of the post-ir irsl signal: new insights for feldspar luminescence dating. *Boreas* 43(4): 780–791, DOI 10.1111/bor.12082.
- Lawson MJ, Roder BJ, Stang DM and Rhodes EJ, 2012. OSL and IRSL characteristics of quartz and feldspar from southern California, USA. *Radiation Measurements* 47(9): 830–836, DOI 10.1016/j.radmeas.2012.03.025.
- Li B and Li SH, 2012. A reply to the comments by Thomsen *et al.* on “luminescence dating of K-feldspar from sediments: a protocol without anomalous fading correction”. *Quaternary Geochronology* 8(1): 49–51, DOI 10.1016/j.quageo.2011.10.001.
- Li GQ, Chen FH, Xia DS, Yang H, Zhang XJ, Madsen DB, Oldknow C, Wei HT, Rao ZG and Qiang MR, 2018. A Tianshan mountains loess-paleosol sequence indicates anti-phase climatic variations in arid central Asia and in East Asia. *Earth and Planetary Science Letters* 494: 153–163, DOI 10.1016/j.epsl.2018.04.052.
- Li G, Duan Y, Huang XZ, Buylaert JP, Wei P, Madsen DB, Rao ZG, She LL and Xie HC, 2016. The luminescence dating chronology of a deep core from Bosten Lake (NW China) in arid central Asia reveals lake evolution over the last 220 ka. *Boreas* 46(2): 264–281, DOI 10.1111/bor.12209.
- Li GQ, Jin M, Wen LJ, Zhao H, Madsen D, Liu XK, Wu D and Chen FH, 2014. Quartz and K-feldspar optical dating chronology of eolian sand and lacustrine sequence from the southern Ulan Buh Desert, NW China: Implications for reconstructing late Pleistocene environmental evolution. *Palaeogeography, Palaeoclimatology, Palaeoecology* 393: 111–121, DOI 10.1016/j.palaeo.2013.11.003.
- Li GQ, Jin M, Duan YW, Madsen DB, Li FL, Yang LP, Wei HT and Chen FH, 2015a. Quartz and K-feldspar luminescence dating of a Marine Isotope Stage 5 megalake in the Juyan Lake Basin, central Gobi Desert, China. *Palaeogeography, Palaeoclimatology, Palaeoecology* 440: 96–109, DOI 10.1016/j.palaeo.2015.08.033.
- Li GQ, Li FL, Jin M, She LL, Duan YW, Madsen DB, Wang LB and Chen FH, 2017. Late quaternary lake evolution in the Gaxun Nur basin, central Gobi Desert, China, based on quartz OSL and K-feldspar pIRIR dating of paleoshorelines. *Journal of Quaternary Science* 32(3): 347–361, DOI 10.1002/jqs.2928.
- Li GQ, Wen LJ, Xia DS, Duan YW, Rao ZG, Madsen DB, Wei HT, Li FL, Jia J and Chen FH, 2015b. Quartz OSL and K-feldspar pIRIR dating of a loess/paleosol sequence from arid central Asia, Tianshan Mountains, NW China. *Quaternary Geochronology* 28(40–53): 40–53, DOI 10.1016/j.quageo.2015.03.011.
- Liu LM, Zhao JF, Zhang JP, Peng WF, Fan JL and Zhang TX, 2013. Water balance Lake Bosten using annual water-budgets method for the past 50 years. *Arid Land Geography* 36(1): 33–40.
- Long H, Habertzettl T, Tsukamoto S, Shen J, Kasper T, Daut G, Zhu L, Mäusbacher R and Frechen M, 2015. Luminescence dating of lacustrine sediments from Tangra Yumco (southern Tibetan Plateau) using post-IR IRSL signals from polymineral grains. *Boreas* 44: 139–152, DOI 10.1111/bor.12096.
- Long H and Shen J, 2015. Underestimated ¹⁴C-based chronology of late Pleistocene high lake-level events over the Tibetan Plateau and adjacent areas: Evidence from the Qaidam Basin and Tengger Desert. *Science China Earth Sciences* 58(2): 183–194, DOI 10.1007/s11430-014-4993-2.
- Long H and Zhang JR, 2016. Luminescence dating of Late Quaternary lake-levels in Northern China. *Quaternary Sciences* 36(5): 1191–1203.
- MadsenDB, Haizhou M, Rhode D, Brantingham PJ and Forman SL, 2008. Age constraints on the late quaternary evolution of Qinghai lake, Tibetan Plateau. *Quaternary Research* 69(2): 316–325, DOI 10.1016/j.yqres.2007.10.013.
- Mejdahl V and Funder S, 1994. Luminescence dating of late Quaternary sediments from east Greenland. *Boreas* 23(4): 525–535.
- McGuire C and Rhodes EJ, 2015. Downstream MET-IRSL single-grain distributions in the Mojave River, southern California: testing assumptions of a virtual velocity model. *Quaternary Geochronology* 30(1): 239–244, DOI 10.1016/j.quageo.2015.02.004.
- Murray AS and Wintle AG, 2000. Luminescence dating of quartz using an improved single-aliquot regenerative-dose protocol. *Radiation Measurements* 32: 57–73, DOI 10.1016/S1350-4487(99)00253-X.
- Murray AS, Olley JM and Caitcheon GG, 1995. Measurement of equivalent doses in quartz from contemporary water-lain sediments using optically stimulated luminescence. *Quaternary Science Reviews* 14(4): 365–371, DOI 10.1016/0277-3791(95)00030-5.
- Murray AS, Thomsen KJ, Masuda N, Buylaert JP and Jain M, 2012. Identifying well-bleached quartz using the different bleaching rates of quartz and feldspar luminescence signals. *Radiation Measurements* 47: 688–695, DOI 10.1016/j.radmeas.2012.05.006.
- Olley JM, Caitcheon GG and Murray AS, 1998. The distribution of apparent dose as determined by optically stimulated luminescence in small aliquots of fluvial quartz: implications for dating young sediments. *Quaternary Science Reviews* 17(11): 1033–1040, DOI 10.1016/S0277-3791(97)00090-5.

- Olley JM, Caitcheon GG and Roberts RG, 1999. The origin of dose distributions in fluvial sediments, and the prospect of dating single grains from fluvial deposits using optically stimulated luminescence. *Radiation Measurements* 30(2): 207–217, DOI 10.1016/S1350-4487(99)00040-2.
- Pessenda LCR, Gouveia SEM and Aravena R, 2001. Radiocarbon dating of total soil organic matter and humin fraction and its comparison with ¹⁴C age of fossil charcoal. *Radiocarbon* 43: 596–601.
- Prescott JR and Hutton JT, 1994. Cosmic ray contributions to dose rates for luminescence and ESR dating: Large depths and long-term time variations. *Radiation Measurements* 23: 497–500, DOI 10.1016/1350-4487(94)90086-8.
- Preusser F, Ramseyer K and Christian S, 2006. Characterisation of low OSL intensity quartz from the New Zealand Alps. *Radiation Measurements* 41(7): 871–877, DOI 10.1016/j.radmeas.2006.04.019.
- Rhodes EJ, 2015. Dating sediments using potassium feldspar single-grain IRSL: initial methodological considerations. *Quaternary International* 362: 14–22, DOI 10.1016/j.quaint.2014.12.012.
- Smedley RK, Duller GAT and Roberts HM, 2015. Bleaching of the post-IR IRSL signal from individual grains of K-feldspar: implications for single-grain dating. *Radiation Measurements* 79: 33–42, DOI 10.1016/j.radmeas.2015.06.003.
- Stokes S, 1992. Optical dating of young (modern) sediments using quartz: results from a selection of depositional environments. *Quaternary Science Reviews* 11(1–2): 153–159, DOI 10.1016/0277-3791(92)90057-F.
- Song YG, Luo D, Du JH, Kang SG, Cheng P, Fu CF and Guo XH, 2018. Radiometric dating of late Quaternary loess in the northern piedmont of South Tianshan Mountains: Implications for reliable dating. *Geological Journal* 53(8): 417–426, DOI 10.1002/gj.3129.
- Stokes S, Bray HE and Blum MD, 2001. Optical resetting in large drainage basins: tests of zeroing assumptions using single-aliquot procedures. *Quaternary Science Reviews* 20(5): 879–885, DOI 10.1016/S0277-3791(00)00045-7.
- Thiel C, Buylaert JP, Murray AS, Terhorst B, Hofer I, Tsukamoto S and Frechen M, 2011. Luminescence dating of the Stratzing loess profile (Austria) – Testing the potential of an elevated temperature post-IR IRSL protocol. *Quaternary International* 234: 23–31, DOI 10.1016/j.quaint.2010.05.018.
- Thomsen KJ, Murray AS, Jain M and Bøtter-Jensen L, 2008. Laboratory fading rates of various luminescence signals from feldspar-rich sediment extracts. *Radiation Measurements* 43(9–10): 1474–1486, DOI 10.1016/j.radmeas.2008.06.002.
- Trauerstein M, Lowick SE, Preusser F and Schlunegger F, 2014. Small aliquot and single grain IRSL and post-IR IRSL dating of fluvial and alluvial sediments from the Pativilca valley, Peru. *Quaternary Geochronology* 22(3): 163–174, DOI 10.1016/j.quageo.2013.12.004.
- Wallinga J, Murray AS and Wintle A, 2000. The single-aliquot regenerative-dose (SAR) protocol applied to coarse-grain feldspar. *Radiation Measurements* 32(5): 529–533, DOI 10.1016/S1350-4487(00)00091-3.
- Wünnemann B, Mischke S and Chen FH, 2006. A Holocene sedimentary record from Bosten Lake, China. *Palaeogeography, Palaeoclimatology, Palaeoecology* 234: 223–238, DOI 10.1016/j.palaeo.2005.10.016.
- Wintle AG, 2008. Luminescence dating: where it has been and where it is going. *Boreas* 37: 471–482, DOI 10.1111/j.1502-3885.2008.00059.x.
- Xiao M, Wu FC, Liao HQ, Li W, Lee XQ and Huang RS, 2010. Characteristics and distribution of low molecular weight organic acids in the sediment pore waters in Bosten Lake, China. *Journal of Environment Science* 22: 328–337.
- Xu Y, Yan S, Jia B and Yang Y, 1996. Numerical relationship between the surface spore-pollen and surrounding vegetation on the southern slope of Tianshan Mountains. *Arid Land Geography* 19: 25–30.
- Yi SW, Buylaert J, Murray AS, Lu HY, Thiel C and Zeng L, 2016. A detailed post-IR IRSL dating study of the Niuyangzigou loess site in northeastern China. *Boreas* 45(4): 644–657, DOI 10.1111/bor.12185.
- Zhang J, Tsukamoto S, Jia Y and Frechen M, 2016. Lake level reconstruction of Huangqihai lake in northern China since MIS 3 based on pulsed optically stimulated luminescence dating. *Journal of Quaternary Science* 31(3): 225–238, DOI 10.1002/jqs.2861.
- Zhao H and Li SH, 2005. Internal dose rate to K-feldspar grains from radioactive elements other than potassium. *Radiation Measurements* 40(1): 84–93, DOI 10.1016/j.radmeas.2004.11.004.